

Study of Effect of Seal Profile on Tribological Characteristics of Reciprocating Hydraulic Seals

S. Bhaumik^a, A. Kumaraswamy^b, S. Guruprasad^a, P. Bhandari^a

^aR & DE (Engineers), Pune, 411015, Maharashtra, India,

^bDefence Institute of Advanced Technology (DU), Pune, 411025, Maharashtra, India.

Key words:

Reciprocating hydraulic seal
Friction
Leakage
Seal wear
Polyurethane seals

ABSTRACT

Effect of seal profile on tribological characteristics such as leakage, friction, and wear in reciprocating hydraulic seals was predicted as a function of number of parameters such as rod velocity, sealed pressure and surface roughness. Experiments were conducted on a specially designed test rig at rod velocities ranging from 0.12-0.5 m/s, oil pressures from 1-20 MPa and rod average surface roughness value from 0.2-0.4 μm . Theoretical analysis was carried out using Greenwood Williamson (GW) model for determining leakage, friction and Archard's equation for evaluating wear in rectangular and U-cup seal profiles. Comparison of theoretically estimated data with experimental results for two seal profiles revealed good agreement. Unlike rectangular seal, back pumping of the fluid was observed in case of U-cup seal. It was also observed that, the performance of U-cup seal profile in terms of leakage, friction and wear was relatively better compared to rectangular seal profile under given set of test parameters.

Corresponding author:

A. Kumaraswamy
Defence Institute of Advanced
Technology (DU),
Pune, 411025,
Maharashtra, India.
E-mail: adepu_kswamy@yahoo.com

© 2015 Published by Faculty of Engineering

1. INTRODUCTION

Hydraulic seals were critical machine elements and sealing performance was of great importance to the quality of the overall system [1,2]. The failure of seals may lead to environmental contamination especially from leakage of toxic fluids. The consequences of seal's malfunction can be quantified by catastrophic failure of a NASA space shuttle 'Challenger' due to cold temperature freezing in 1986. Variety of seals have been developed and tested over last four decades. However, initial seal designs were based on trial and error

method and earlier test rigs were not equipped with necessary data acquisition system for testing seal performance under static and dynamic conditions [3]. The sealing contact in reciprocating hydraulic seals typically consists of a thin lubricating film that separates the seal from the rod. The mathematical model to obtain flow rate was derived from Navier-Stokes equation that account for forces acting on a fluid element. One dimensional Reynold's equation also called as inverse hydrodynamic theory was used to determine thickness of the fluid film, which was validated by experimental results [4-6]. One dimensional Reynold's equation and

elastic displacement equations were solved simultaneously with iterative process, which was called as direct method [7]. This method was extensively used by numerous investigators; however, it has certain limitations such as convergence of large deformations and more computational time. The physics behind the sealing behavior was described by a numerical model [8]; however, the results were not validated by the experimental results. Subsequently, investigation was extended to the performance of simple seal structure in terms of leakage, pumping rate and film thickness on the rod surface [9]. Seal wear is another important factor affecting the performance of hydraulic seals.

Experimental analysis of one of the seal materials i.e. EPDM (Ethylene Propylene Diene Monomer) rubber revealed that, hardness significantly affects the flow behavior and wear characteristics. Hardness in turn depends on the proportion of carbon black (CB) indicating that, the flow behavior can be controlled by CB concentration in the rubber [10]. There exist several theories for modelling wear taking the fracture or the fatigue properties into account [11]. The first trials on theoretical and numerical calculations of wear profiles were carried out [12]. A method for simulating seal wear in which the contact pressure was obtained from Finite Element (FE) model and nodal wear increment was proposed [13]. This was the most widely used method in which the displacement of contact nodes was based on the nodal wear increments [14]. This method was further refined to account for heat generation and time dependent material properties during the wear simulation [15].

Unlike O-ring seals, rectangular seals do not flex under cyclic pressures and are less prone to leakage due to flexing and wear. Therefore, rectangular seals are widely used in heavy duty hydraulic equipment like linear actuators of earth moving equipment, defence equipment and in industrial automation. On the other hand, U-cup seal profiles are used in hydraulic actuators involving higher sliding velocities. The cross section of U-cup seal profile is larger compared to rectangular seal profile facilitating deflections of the piston rod and changes in pressure.

Several studies have been carried out on friction characteristics of seals [16-18], however, limited literature is available on effect of seal profile on tribological characteristics in terms of friction, leakage and seal wear of reciprocating hydraulic seals. In order to fill up this gap albeit partially, an attempt was made in the present investigation to understand the behavior of polyurethane seals of rectangular and U-cup seal profiles at different sealed oil pressures, rod velocities and surface roughness values. It was observed that, the U-cup seal profile exhibited back pumping phenomenon, relatively less friction and wear compared to rectangular seal under given set of test conditions as mentioned in Table 1. It was also noted that, there is a good agreement between theoretically computed data and experimentally measured values and the effect of seal profile is apparent on the performance characteristics of seals.

2. EXPERIMENTAL PROCEDURE

A new test rig has been designed and developed to measure friction; leakage and seal wear [19]. An efficient alternative method [20] for testing and qualifying large diameter piston rod seals has been considered rather than conventional tests, in which seals are tested as part of complete hydraulic cylinder assembly. The test setup designed as per ISO 7986 is shown in Fig.1 [21]. A set of two seals (rectangular or U-cup profile) will isolate the inside chamber that was initially charged to the sealed oil pressure. Friction was measured with the help of a load cell between the test and articulating cylinders. The floating piston supporting weight 'W' maintains the test pressure. Any leakage or back pumping can be measured by recording the displacement of floating piston with the help of a dial gauge as illustrated in Fig. 1 (b).

The test fluid temperature was measured by a temperature transducer HYDAC ETS 4548-H-000 capable of sensing the temperature in the range of -250 to 1000 °C and accuracy of ± 1.5 %. The test cylinder circuit consists of high pressure hydraulic pump integrated with a relief valve, heat exchanger and temperature controller to control the temperature of fluid in the test chamber.

During the test, the reciprocating motion of rod was obtained by an articulating cylinder and velocity of rod was controlled by an electronic controller. The minimum speed of the actuator was limited to 0.12 m/s based on minimum pump flow rate possible. The sealed oil pressure was considered in the range of 1-20 MPa that was within the normal working pressure existing in any hydraulic system. The leakage was measured using a measuring tube for a given number of cycles. Reduction in weight of seal after every 200 cycles was considered as a measure of seal wear. The test parameters considered in the present study were mentioned in Table 1.



Fig. 1(a) Seal Test Rig.

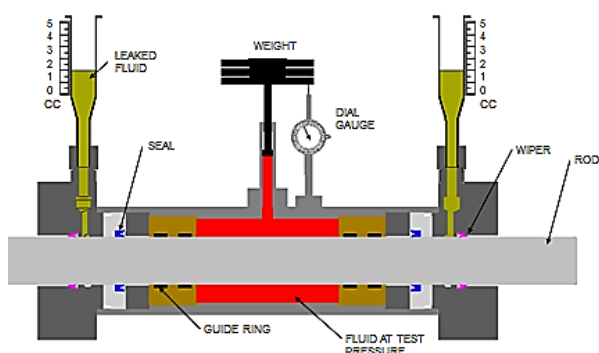


Fig. 1(b) Schematic illustrating leakage measurement.

Table 1. Test parameters considered in the study.

Test parameter	Rectangular seal	U-cup seal
Inner diameter, mm	Ø36	RS036, ROTAMIC make
Outer diameter, mm	Ø46	
Seal width, mm	6	
Gland groove inner diameter, mm	Ø45	Ø45.9
Seal material	Polyurethane (shore hardness A90)	
Seal's pre-compression after assembly	10 %	
Test temperature	30 °C	
Sealed oil pressure, MPa	1, 10, 15 and 20	
Rod speed, m/s	0.12, 0.2, 0.3, 0.4 and 0.5	
Rod average surface roughness, R_a , μm	0.2 and 0.4	
Steel rod outer diameter, mm	Ø36	

3. FINITE ELEMENT ANALYSIS (FEA)

An axisymmetric FE model for rectangular and U-cup seal profiles with hybrid formulation using ABAQUS is shown in Fig. 2. The CAX4RH element was used for seal and CAX4R element for rod and gland. In any numerical approach, the number of nodes or in other words number of elements considered in the model generally has a direct effect on the results. Therefore, a mesh convergence study has been carried out by increasing number of mesh elements from 10000 to 15000 in steps of 200. No significant change in results was observed beyond 12600 elements; therefore, simulations were carried out considering 12600 elements to reduce the computational effort.

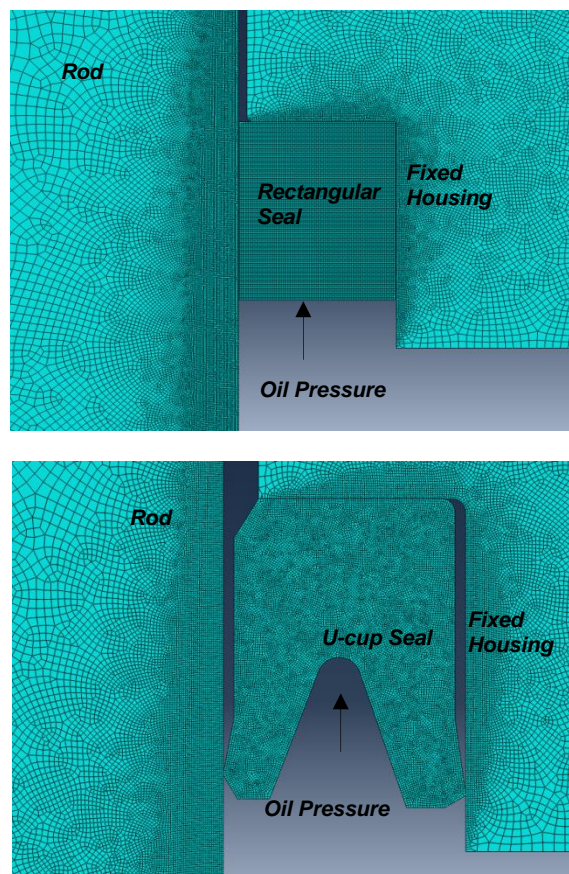


Fig. 2. Axisymmetric FE model for rectangular and U-cup seal.

Elastomeric seals fall under both geometric as well as material nonlinear category. Finite deformation theory will account for geometric nonlinear aspect and theory of hyper elasticity will consider the nonlinear stress versus strain behavior. Uni-axial and bi-axial tension, planar and volumetric shear tests were to be carried out to understand the material nonlinearity. The

test results can be fitted to different theoretical models such as Mooney-Rivlin, Ogden, Yeoh etc. to determine the required constants that describe a particular model. The first order strain energy function for a hyper-elastic Mooney-Rivlin model was described as:

$$W = C_1(\bar{I}_2 - 3) + C_2(\bar{I}_1 - 3) + D_1(J - 1)^2$$

where, $\bar{I}_1 = J^{-\frac{2}{3}}I_1$ and $\bar{I}_2 = J^{-\frac{4}{3}}I_2$ in which, I_1 and I_2 were the first and second invariants of right Cauchy Green deformation tensor described as, $I_1 = \lambda_1^2 + \lambda_2^2 + \lambda_3^2$; $I_2 = \lambda_1^2\lambda_2^2 + \lambda_2^2\lambda_3^2 + \lambda_3^2\lambda_1^2$ in which, $\lambda_1, \lambda_2, \lambda_3$ were stretch ratios; $J = |F|$, for an incompressible material the value of $J = 1$. Constants C_1, C_2 given in Table 2 can be obtained by curve fitting of the experimental data. These formulations were included in ABAQUS software in the form of algorithms. Poisson's ratio of 0.495 was considered for incompressible seal material.

Table 2. Mooney-Rivlin model.

Polyurethane	Temp (°C)	C1 (MPa)	C2 (MPa)	D1
	30	0.2	6	0.0096

4. ESTIMATION OF LEAKAGE, FRICTION AND SEAL WEAR

The Reynold's equation obtained by considering the mass flux balance within the fluid element was used to determine the fluid film thickness. This value of film thickness was substituted in the non-dimensionalised Navier-Stokes equations to determine flow rate or leakage of the fluid. Further, modified Reynold's equation that also accounted for cavitation and surface roughness was used to obtain the accurate value of fluid flow rate.

This theory was also used to calculate the film thickness from the contact pressure distribution obtained from FEA. Fluid pressure and film thickness at seal/rod interface was assumed to be governed by one-dimensional Reynold's equation given by inverse hydrodynamic lubrication (IHL) theory [22] described as:

$$\frac{d}{dx} \left(\frac{h^3}{\eta} \frac{dp_{dc}}{dx} \right) = 6U \frac{dh}{dx} \tag{1}$$

where, h is the film thickness.

4.1 Estimation of leakage

Leakage was calculated from eq. (2) given below, [22]:

$$\dot{Q} = \pi D \left(-\frac{h_a^3}{12\eta} \frac{\partial p_{dc}}{\partial x} + U \frac{h_a}{2} \right) \tag{2}$$

Total leakage for a given number of cycles can be determined by multiplying eq. (2) by number of cycles and stroke length upon velocity. Hence, the net leakage per stroke can be written as [23]:

$$Q = \pi DS(h_{i_outstroke} - h_{i_instroke}) \tag{3}$$

Total leakage can be found out by multiplying eq. (3) by number of cycles. However, eq. (2) and eq. (3) do not account for surface roughness. Therefore, the amount of leakage calculated was of very low as explained later under sec. 5. Oil gets entrapped into the troughs of the asperities on the rod surface that will be transported out of the actuator. The fluid pressure may fall below vapour pressure due to which the fluid film may contain vapor bubbles [24]. The film thickness may vary depending on the nature of contact i.e. surface roughness of rod and the seal as shown in Fig. 3.

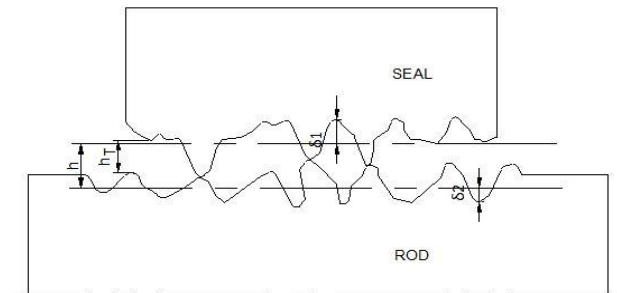


Fig. 3. Surface roughness of the rod and the seal.

The truncated (local) film thickness, $h_T = h + \delta_1 + \delta_2$ where δ_1, δ_2 are random heights of the seal and rod surfaces defined from mean level of the surfaces. They are assumed to have Gaussian distribution of heights with zero mean and s_1, s_2 as the standard deviations. The combined roughness $\delta = \delta_1 + \delta_2$ has a variance $s^2 = s_1^2 + s_2^2$. The average truncated film thickness was defined as, $\bar{h}_T = \int_{-h}^{\infty} (h + \delta)f(\delta)d\delta$, where, $f(\delta)$ was the probability density function of δ . The generalized Reynold's equation that includes cavitation and surface roughness was considered by Greenwood Williamson (GW) [24] as given below,

$$\frac{\partial}{\partial \hat{x}} \left(\phi_{xx} H^3 e^{-\hat{\alpha} F \phi} \frac{\partial}{\partial \hat{x}} (F\phi) \right) = 6\zeta \frac{\partial}{\partial \hat{x}} \left(\{1 + (1 - F)\phi\} \{H_T + \phi_{scx}\} \right) \quad (4)$$

$$\left. \begin{array}{l} \text{In the liquid region: } \phi \geq 0, F = 1 \text{ and } P = \phi, \\ \text{In the cavitated region, } \phi < 0, F = 0 \text{ and } P = 0, \\ \text{on the oil side i.e. at } \hat{x} = 0, \hat{p} = 1 + \phi, P = P_{sealed}, \\ \text{and on the air side i.e. at } \hat{x} = 1, P = 1. \end{array} \right\} \quad (5)$$

The flow factors ϕ_{xx}, ϕ_{scx} were incorporated to account for the effect of surface roughness values. A method has been developed by N. Patir, H.S. Cheng to obtain the flow factors ϕ_{xx} using numerical simulation [25-26]. They had performed a series of numerical analyses in which the Reynold's equation containing the local film thickness was solved for a variety of randomly generated roughness patterns. Total flow was composed of Poiseuille flow i.e. LHS of eqn. (4) and Couette flow i.e. RHS of eqn. (4). Therefore, total flow rate can be written as:

$$\hat{q} = - \left(\phi_{xx} H^3 e^{-\hat{\alpha} F \phi} \frac{\partial}{\partial \hat{x}} (F\phi) \right) + 6\zeta \frac{\partial}{\partial \hat{x}} \left(\{1 + (1 - F)\phi\} \{H_T + \phi_{scx}\} \right) \quad (6)$$

4.2 Estimation of friction

The average fluid shear stress taking cavitation effects into account were given below [24]:

$$\hat{\tau}_f = \frac{\tau_f - \hat{\sigma}}{E \xi} e^{\hat{\alpha} F \phi} \frac{\zeta}{H} (\phi_f - \phi_{fss}) - \phi_{fpp} \frac{\hat{\sigma} H}{\xi} \frac{\partial}{\partial \hat{x}} (F\phi) \quad (7)$$

where, ϕ_f, ϕ_{fss} and ϕ_{fpp} were the shear stress flow factors [25-26]. The asperity contact pressure was defined using eq. (8) [24],

$$P_c = \frac{4}{3} \frac{\hat{\sigma}^{3/2}}{(1-\theta^2)} \frac{1}{\sqrt{2\pi}} \int_H^\infty (z - H)^{3/2} e^{-z^2/2} dz \quad (8)$$

The contacting asperities at rod/seal interface causes frictional shear stress that was given by eq. (9) [24]:

$$\hat{\tau}_c = \frac{\tau_c}{E} = -f P_c \left(\frac{\zeta}{|\zeta|} \right) \quad (9)$$

The net frictional force between the seal and the rod was obtained by adding eq. (7) and eq. (9).

$$F = \pi D \int_0^L (\tau_f + \tau_c) dx \quad (10)$$

4.3 Computation procedure

(a) Assuming initial value of H eqn. (4) was solved for ϕ and F , considering boundary conditions in eqn. (5) using finite volume

method. Thus, fluid pressure distribution P_{def} and cavitation zones were found.

(b) P_c was calculated using eq. (8) and H value was calculated and refined as mentioned below:

$H = H_d + H_{def}$, where H_d was the dry film thickness i.e. the thickness that a hypothetical film would occupy under dry contact conditions (in the absence of any fluid pressure). H_d was calculated by equating P_{dc} (calculated from FEA) to P_c and curve fitting to invert eq. (8). H_{def} was the radial deformation of the sealing edge, when a net pressure $P_{def} + P_c - P_{dc}$ was applied on the sealing edge.

(c) The average truncated film thickness was:

$$\text{given by, } H_T = \frac{H}{2} + \frac{H}{2} \operatorname{erf} \left[\frac{H}{\sqrt{2}} \right] + \frac{1}{\sqrt{2\pi}} e^{-\frac{H^2}{2}}$$

(d) Steps (b)-(c) were repeated for convergence.

(e) Eq. (6) was used to obtain total flow rate \hat{q} and friction was obtained using eq. (10).

4.4 Estimation of wear

Wear is defined as the removal of material from the surface due to mechanical or chemical processes. The wear due to mechanical behavior can be classified as a) Asperity deformation and removal b) Plowing of the surface c) Delamination d) Adhesive e) Abrasion f) Fretting and g) Solid particle impingement. These processes lead to mild or severe wear (rough and torn surfaces). Archard's model given by eq. (11) is widely used out of several wear models available and is described as under.

$$\dot{w} = \frac{K}{H_b} F U \quad (11)$$

where, \dot{w} is rate of change of wear, K is wear coefficient, H_b is Brinell hardness number of seal material, F is cavitation index and U is the rod velocity. Often measured worn out volumes vary in direct proportion with the total sliding distances and the applied loads over certain load ranges. Abrupt changes in wear rates (wear transition) are observed at specific critical loads. Such changes are the result on the complex interplay between the softening and chemically reacting behaviors of the material induced by high flash temperatures. Abrupt increase in wear rates are commonly found at high loads and these are often associated with welding and seizure. However, in some cases these high wear

rates may revert to low values even at higher loads. Measured values of K are frequently small and ranges from 10^{-8} for incompatible metal scrubbing against each other with good lubrication to 10^{-3} for clean unlubricated surfaces like metals. The magnitude of these values together with the original interpretation of K given above suggest a probabilistic interpretation of the wear coefficient that represents the fraction of the actual contact surface, which was actually removed by the wear process. It will also represent the probability that any given individual friction contact event culminates with the breakage and removal of a wear particle.

5. RESULTS AND DISCUSSION

FE Analysis was carried out as described under section 3 for sealed pressure ranging from 1-20 MPa, rod velocities ranging from 0.12-0.5 m/s before the leakage was measured experimentally. It was observed that, the change in seal contact pressure on rod with rod velocity was not significant. Leakage predicted by eqn. (4) and (5) was identical and the magnitude of leakage/ back pumping was very small, since both the approaches were based on IHL theory, which do not account for the surface roughness. The results from GW model were more realistic because the surface roughness was also accounted for. The experimental results were slight deviating from theoretical analysis data due to the following reasons.

- Friction, leakage and wear theories were independently considered at steady flow and constant sealed pressure.
- Viscous heating of oil and seal due to friction were not solved using coupled displacement temperature analysis.
- Seal's visco-elasticity was not considered in the FE model.

5.1 Net leakage/back pumping for 500 cycles

Increase in sealed oil pressure from 1 to 20 MPa resulted in slight reduction in the net leakage through rectangular seal as shown in Fig. 4 due to increase in contact pressure at seal/rod interface. The increase in contact pressure causes the seal to deform into the gap between the crests and troughs at the interface, which in

turn decreases the fluid film thickness and leakage. Fluid flow rate was proportional to the velocity as described by IHL and GW models. For rectangular seal, the pressure driven Poiseuille flow was smaller (independent of rod velocity) than the Couette flow (directly proportional to rod velocity). The total flow (constant Poiseuille flow and increasing Couette flow) increased as a function of rod speed.

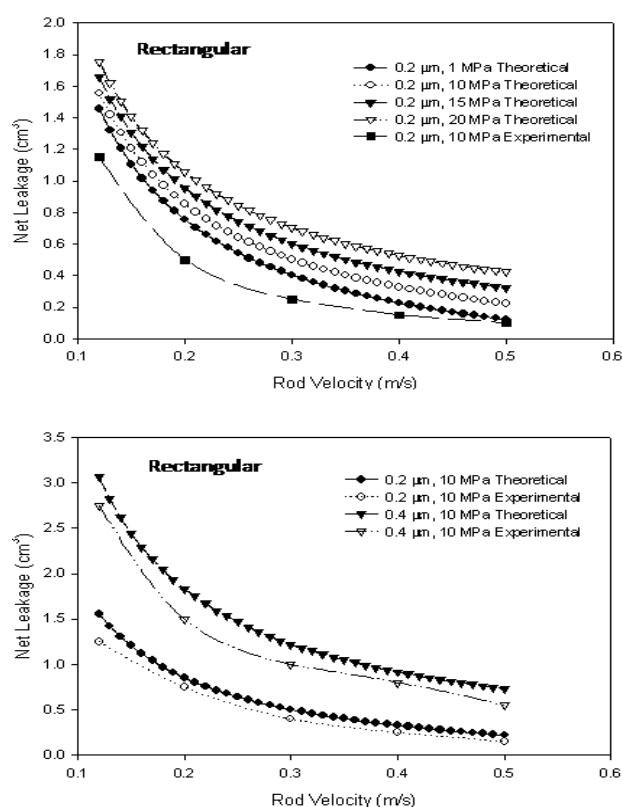


Fig. 4. Net leakage through rectangular seal vs. rod velocity for 500 cycles.

On the other hand, increase in the rod's surface roughness from 0.2 to 0.4 μm found to increase the net leakage due to fluid entrapment into the valleys on the rod. Increase in sealed oil pressure reduced net leakage (i.e. increased back pumping) in U-cup seal as shown in Fig. 5 due to the fact that, the fluid flow rate was proportional to the velocity as described by IHL and GW models. For U-cup seal, the pressure driven Poiseuille flow was large and negative (independent of rod velocity) than the Couette flow (directly proportional to rod velocity) unlike rectangular seal. The total flow (constant Poiseuille flow and increasing Couette flow) increased with rod velocity, which was identical with rectangular seal. The increase in the surface rod's roughness from 0.2 to 0.4 μm resulted in increase in back pumping.

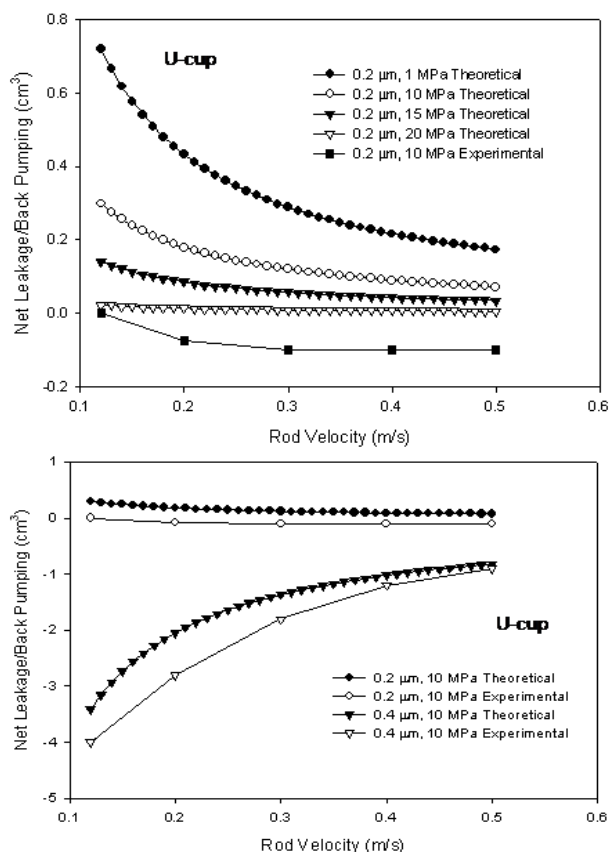


Fig. 5. Back pumping through U-cup seals Vs rod velocity for 500 cycles.

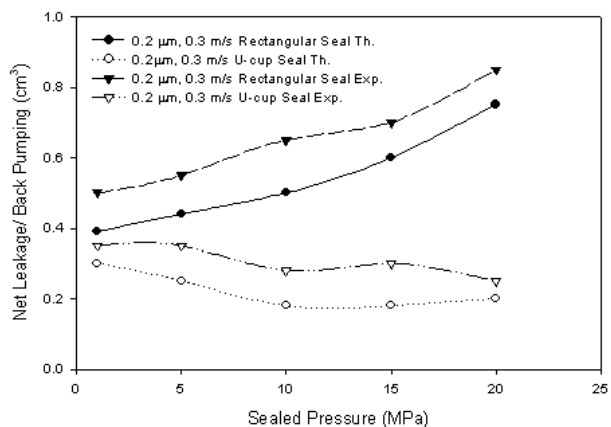


Fig. 6. Effect of seal profile on leakage Vs sealed pressure (0.2 μm, 0.3 m/s, 500 cycles).

Effect of seal profile on leakage Vs sealed pressure at constant surface roughness (0.2 μm) and rod velocity (0.3 m/s) for 500 cycles was shown in Fig. 6. As mentioned earlier in this section, net leakage for rectangular seal slightly reduced with increase in sealed pressure and for U-cup seal, back pumping was increased with increase in sealed pressure. This was due to the fact that, the contact area of the U-cup seal was smaller at low sealed pressures compared to high sealed pressures. At higher pressures the

pressure driven flow increased and the velocity driven flow was considered as constant. Therefore, there was an increase in back pumping.

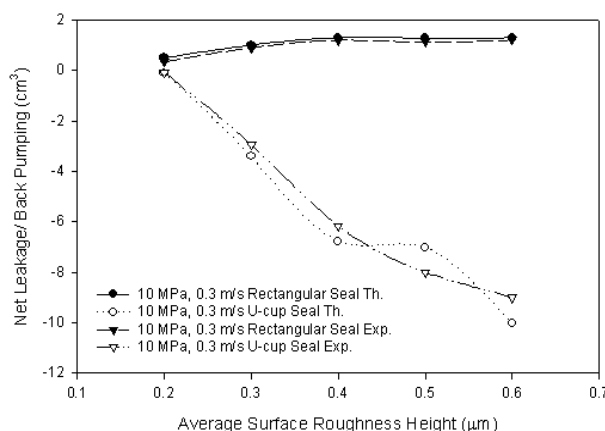


Fig. 7. Effect of seal profile on leakage Vs sealed pressure (10 MPa, 0.3 m/s, 500 cycles).

Effect of seal profile on leakage Vs sealed pressure at constant sealed pressure (10 MPa) and rod velocity (0.3 m/s) for 500 cycles was shown in Fig. 7. As mentioned previously, net leakage/back pumping for both seals increased with increase in the rod's surface roughness due to more entrapment of oil in the valleys.

5.2 Estimation of frictional force

Frictional force vs. rod velocity for rectangular seal for a constant surface roughness (0.2 μm) and varying oil pressure (1-20 MPa) was shown in Fig. 8. It may be noted that, with increase in oil pressure the contact pressure of the seal increases this in turn causes increase in frictional force.

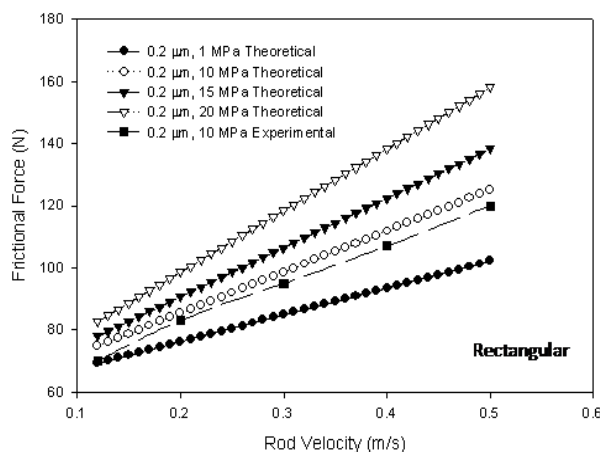


Fig. 8. Frictional force vs. rod velocity for rectangular seal.

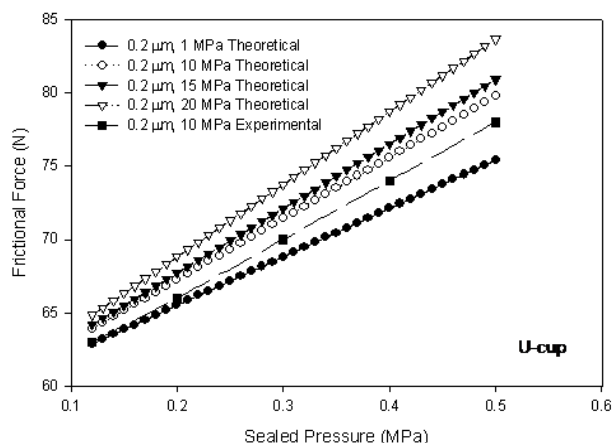


Fig. 9. Frictional force vs. sealed pressure for U-cup seal.

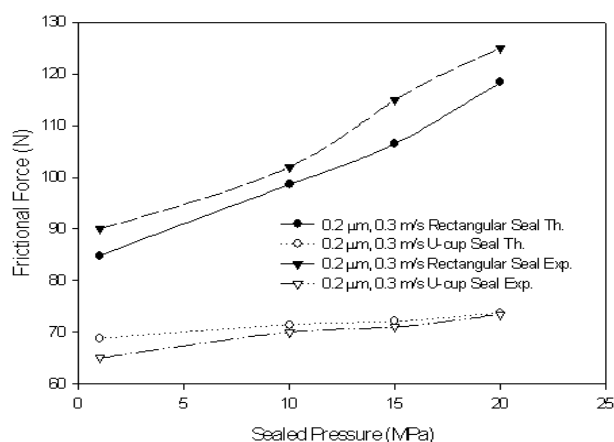


Fig. 10. Effect of seal profile on frictional force vs. sealed pressure (0.2 μm, 0.3 m/s).

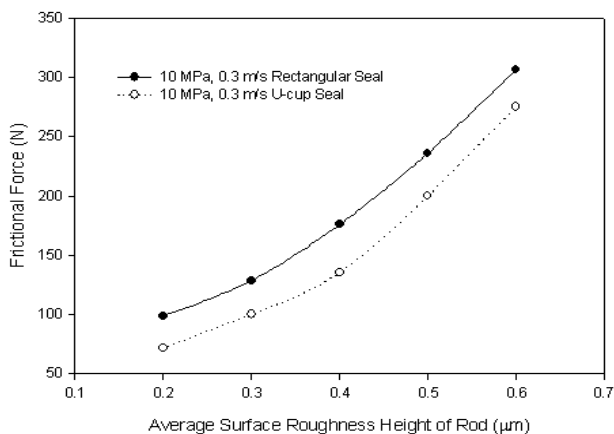


Fig. 11. Effect of seal profile on frictional force vs. average surface roughness (10 MPa, 0.3 m/s).

The frictional force increased with increase in rod velocity due to thinning of fluid film at seal/rod interface at increased rod velocities. Frictional force vs. rod velocity behavior in case of U-cup seal was similar to that of rectangular seal. However, the value of the frictional force in U-cup seal was significantly lower compared to rectangular seal as shown in Fig. 9. Further,

there was a good agreement between experimental and theoretical results as shown in Figs. 8 and 9.

Effect of seal profile on frictional force vs. sealed pressure for constant surface roughness (0.2 μm) and rod velocity (0.3 m/s) was plotted in Fig. 10. Effect of seal profile on frictional force vs. average surface roughness for constant sealed pressure (10 MPa) and rod velocity (0.3 m/s) was shown in Fig. 11. It was observed that, frictional force increased with increase in sealed pressure and increase in surface roughness value for both the profiles due to increase in contact area. Rectangular seal indicated more frictional force compared to U-cup seal and the experimental values correlates well with the theoretical results.

5.3 Seal wear for 2000 cycles

Effect of seal profile on seal wear vs. rod velocity and seal wear vs. sealed pressure for 2000 cycles was plotted in Fig. 12 and Fig. 13 respectively.

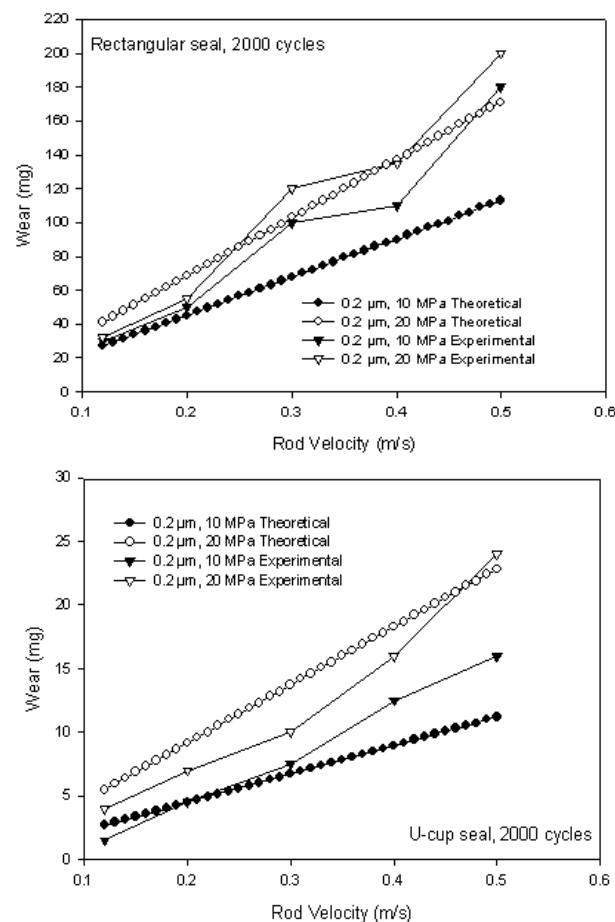


Fig. 12. Effect of seal profile on seal wear vs. rod velocity.

It was observed that, the seal wear increased with increase in rod velocity and increase in sealed oil pressure. This may be attributed to abrasion or plowing of seal surface and reduced lubrication at higher contact pressures and velocities at the seal/rod interface in both the seals.

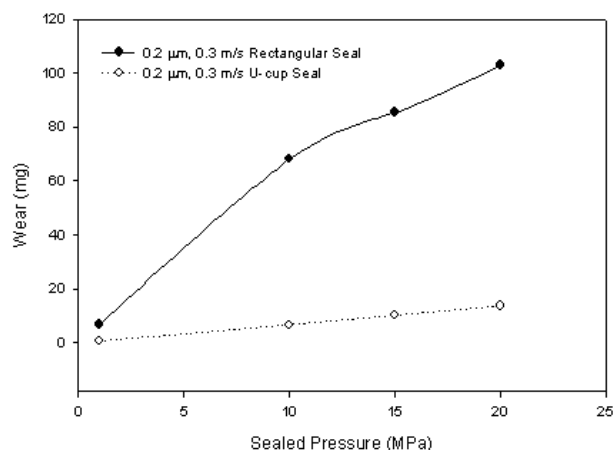


Fig. 13. Effect of seal profile on seal wear vs. sealed pressure for 2000 cycles.

The wear coefficient depends on the severity of the wear. The wear coefficient is high of the order of 10^{-2} , if the seal wear is severe while for mild seal wear, the wear coefficient is relatively low of the order of 10^{-10} . Sliding contact at high loads and velocities results in severe wear leading to sizeable surface damage and large scale material transfer. Seal-metal contact is considered as a severe wear; therefore wear coefficient of 2×10^{-2} has been used in the study. Experimental values of wear indicated good correlation with the theoretical values. The magnitude of wear was significantly higher in case of rectangular seal profile compared to U-cup seal profile indicating the effect of seal profile on seal wear as shown in Fig. 13.

6. CONCLUSIONS

1. For U-cup seal, the pressure driven Poiseuille flow was large and negative than the Couette flow unlike rectangular seal. The total flow (constant Poiseuille flow and increasing Couette flow) increased with rod velocity, which was identical with rectangular seal.
2. The increase in surface rod's roughness from 0.2 to 0.4 μm resulted in increase in back pumping.

3. Frictional force as a function of rod velocity and sealed pressure for U-cup seal was similar to that of rectangular seal. However, the value of the frictional force in U-cup seal was significantly lower compared to rectangular seal.
4. The seal wear increased with increase in rod velocity and increase in sealed oil pressure. This may be attributed to abrasion or plowing of seal surface and reduced lubrication at higher contact pressures and velocities at the seal/rod interface in both the seals.
5. There was a good agreement between theoretically computed values of leakage, friction and wear with the corresponding experimental values.
6. Comparison of the results reveals that, performance of U-cup seal in terms of leakage, friction and wear was relatively superior compared to rectangular seal under same set of test conditions.

Acknowledgements

The authors would like to extend thanks to Mr. Rakesh, Mr. Abhishek Kumar, Mr. CK Waghmare and Mr. ManojBhujbal of R&DE (Engrs), Pune, India for providing assistance during the course of work. One of the authors Mr. Shankar Bhaumik would like to thank Vice Chancellor, DIAT (DU), Pune for permitting him to do PhD.

Nomenclature

D	Rod diameter, mm
E	Modulus of elasticity of rubber, MPa
f	Friction coefficient for asperity contact
F	Cavitation index
h	Film thickness, mm
H	Dimensionless film thickness, h/σ
H_b	Brinell hardness number
K	Wear coefficient, $10^{-8}\text{mm}^3/\text{Nm}$
L	Length of seal in reciprocating direction, mm
N	Asperity density, 10^{14}m^{-2}
P	Dimensionless fluid pressure, p/p_a
p_a	Ambient pressure, Pa
P_c	Dimensionless asperity contact pressure, p_c/E
P_{dc}	Dimensionless dry contact pressure, p_{dc}/E
P_{def}	Dimensionless fluid pressure for deformation analysis, $P(p_a)/E$

\hat{q}	Dimensionless flow rate per unit circumferential length, $(12\eta qL/p_a\sigma^3)$
R	Asperity radius, μm
S	Stroke, m
U	Rod velocity, m/s
\dot{w}	Rate of change of wear, mm^3/s
\hat{x}	Dimensionless axial co-ordinate, x/L
α	Pressure-viscosity coefficient, 10^{-9}Pa^{-1}
$\hat{\alpha}$	Dimensionless pressure-viscosity coefficient, α_a
η	Dynamic viscosity of oil, Pa·s
ν	Seal's Poisson's ratio
Φ	Fluid pressure/density function,
$\Phi_f, \Phi_{fss}, \Phi_{fpp}$	Shear stress factors
Φ_{xx}, Φ_{scx}	Flow factors
$\hat{\rho}$	Dimensionless density, ρ/ρ_1
ρ_1	Density of oil, kg/m^3
σ	Average roughness height, μm
$\hat{\sigma}$	Dimensionless roughness, $(\sigma N^{2/3}R^{1/3})$
ξ	$R^{1/3}N^{2/3}EL/p_a$
ζ	Dimensionless rod speed, $\eta UL/(p_a\sigma^2)$

REFERENCES

- [1] S. Jianjun, G. Boqin and W. Long, 'Discussion on controllability of mechanical seal and its engineering application', *Chinese Journal of Mechanical Engineering*, vol. 41, no. 2, pp. 15-19, 2005.
- [2] Z. Jianfeng, 'Study on thermo-hydrodynamic effect in mechanical seals', *Ph.D thesis*, Nanjing: Nanjing University of Technology, 2006.
- [3] Parker Hannifin, *O-ring Handbook*. Cleveland, OH, 2001.
- [4] C.M. White and D.F. Denny, *The sealing mechanism of flexible packing*, Scientific and Technical Memorandum. 3/47, UK Ministry of Supply, 1947.
- [5] H. Blok, *Inverse problems in hydrodynamic lubrication and design directives for lubricated flexible surfaces*. Proc. Int. Symposium on Lubrication and Wear, 1963, Houston, TX, USA
- [6] A.F.C Kanters, J.F.M Verest and M. Visscher, 'On reciprocating elastomeric seals: calculation of film thicknesses using the inverse hydrodynamic lubrication theory', *Tribological Transactions*, vol. 33, no. 3, pp. 301-306, 1990.
- [7] G.K. Nikas, 'Elasto hydrodynamics and mechanics of rectangular elastomeric seals for reciprocating piston rods', *J. of Tribology*, vol. 125, no. 1, pp. 60-69, 2002.
- [8] R.F. Salant, N. Maser and B. Yang, 'Numerical model of a reciprocating hydraulic rod seal', *ASME J. Tribol.*, vol. 129, no. 1, pp. 91-97, 2006.
- [9] L. Hörl, W. Haas and U. Nifßler, 'A comparison of test methods for hydraulic rod seals', *Sealing Technology*, vol. 2009, no. 12, pp. 8-13, 2009.
- [10] A. Mukhopadhyay, 'Some tribological characterization of 'EPDM' rubber', *Tribology in Industry*, vol. 36, no. 2, pp. 109-116, 2014.
- [11] H.C. Meng and K.C. Ludema, 'Wear Models and Predictive Equations: Their Form and Content', *Wear*, Vol. 181-183, no. 2, pp. 443-457, 1995.
- [12] G.L. Galin and I.G. Goryacheva, 'Contact problems and their applications in the theory of friction and wear', *Trenieilznos*, vol. 1, pp. 105-119, 1980.
- [13] J.F. Archard, 'Contact and rubbing of flat surface', *J. Applied Physics*, vol. 24, no. 8, pp. 981-988, 1953.
- [14] P. Pödra and S. Andersson, 'Simulating sliding wear with finite element method', *Tribology International*, vol. 32, no. 2, pp. 71-81, 1999.
- [15] L. Kónya and K. Váradi, 'Wear simulation of a polymer-steel sliding pair considering temperature and time-dependent material properties', *Tribology of Polymeric Nanocomposites, Tribology and Interface Engineering Series*, vol. 55, pp. 130-145, 2008.
- [16] M. Visscher and A.F.C. Kanters, 'Literature review and discussion on measurements of leakage lubricant film thickness and friction of reciprocating elastomeric seals', *STLE Lubr. Eng.*, vol. 46, no. 12, pp. 785-791, 1990.
- [17] I. Demirci, S. Mezghani, M. Yousfi, H. Zahouani and M.E. Mansori, 'The scale effect of roughness on hydrodynamic contact friction', *Tribological Transactions*, vol. 55, no. 5, pp. 705-712, 2012.
- [18] C. Cristescu, C. Dumitrescu, R. Radoi and L. Dumitrescu, 'Experimental research for measuring friction forces from piston sealing at the hydraulic cylinders', *Tribology in Industry*, vol. 36, no. 4, pp. 465-474, 2014.
- [19] S. Bhaumik, A. Kumaraswamy and S. Guruprasad, 'Design & development of test rig for investigation of contact mechanics phenomena in reciprocating hydraulic seals', *Procedia Engineering*, vol. 64, pp. 835-843, 2013.
- [20] L. Boni, 'Piston rod Seals and related efficient testing', *National Fluid Power Association*, vol. 108-23.2, pp. 627, 2008.
- [21] ISO 7986: *Hydraulic fluid power-sealing devices - standard test methods to assess the performance of seals used in oil hydraulic reciprocating applications*, 1997.

- [22] A. Fatu and M. Hajjam, 'Numerical modeling of hydraulic seals by inverse lubrication theory', *Proceedings of the Institution of Mechanical Engineers, Part J: Journal of Engineering Tribology*, vol. 225, no. 12, pp. 1159-1173, 2011.
- [23] J. Mao, W. Wang and Y. Liu, 'Experimental and theoretical investigation on the sealing performance of the combined seals for reciprocating rod', *J. of Mech. Sc. and Tech*, vol. 26, no. 6, pp. 1765-1772, 2012.
- [24] A. Thatte and R.F. Salant, 'Elastohydrodynamic analysis of an elastomeric hydraulic rod seal during fully transient operation', *ASME Journal of Tribology*, vol. 131, no. 3, pp. 1-11, 2009.
- [25] N. Patir and H.S. Cheng, 'An Average Flow Model for Determining Effects of Three-Dimensional Roughness on Partial Hydrodynamic Lubrication', *Journal of Lubrication Technology-Transactions of the ASME*, vol. 100, no. 1, pp. 12-17, 1978.
- [26] N. Patir and H.S. Cheng, 'Application of Average Flow Model to Lubrication between Rough Sliding Surfaces', *Journal of Lubrication Technology-Transactions of the ASME*, vol. 101, no. 2, pp. 220-230, 1979.